Available online at www.sciencedirect.com
ScienceDirect
Bioresource Technology 99 (2008) 7742–7749
BIORESOURCE TECHNOLOGY

Design and analysis of a solar reactor for anaerobic wastewater treatment

Andreas Ch. Yiannopoulos [a], Ioannis D. Manariotis [b], Constantinos V. Chrysikopoulos [b,*]

[a] Department of Mechanical Engineering, Technological and Educational Institute of Patras, M. Alexandrou 1, 26334 Patras, Greece
[b] Environmental Engineering Laboratory, Department of Civil Engineering, University of Patras, 26500 Patras, Greece

Received 23 April 2007; received in revised form 20 January 2008; accepted 27 January 2008
Available online 6 March 2008

Abstract

The aim of this research was to design a solar heated reactor system to enhance the anaerobic treatment of wastewater or biological sludge at temperatures higher than the ambient air temperature. For the proposed reactor system, the solar energy absorbed by flat plate collectors was transferred to a heat storage tank, which continuously supplied an anaerobic-filter reactor with water at a maximum temperature of 35 °C. The packed reactor was a metallic cylindrical tank with a peripheral twin-wall enclosure. Inside this enclosure was circulated warm water from the heat storage tank. Furthermore, a mathematical model was developed for the prediction of the temperature distribution within the reactor under steady state conditions. Preliminary results based on model simulations performed with meteorological data from various geographical regions of the world suggested that the proposed solar reactor system could be a promising and environmentally friendly approach for anaerobic treatment of wastewater and biological sludge.

Keywords: Solar energy; Solar water heating; Biological treatment; Anaerobic filter; Municipal wastewater

1. Introduction

The anaerobic stabilization of sludge produced from the treatment of municipal and agro-industrial wastewaters is a well established technology (Metcalf and Eddy, 2003; McCarty, 1982; Switzenbaum, 1995). Furthermore, the anaerobic treatment of municipal wastewater is increasingly used more often, especially in warm climate areas, because of its low energy requirements. Anaerobic treatment, compared to conventional aerobic treatment, requires lower capital and operation costs, yields lower production of stabilized sludge, but achieves lower removal efficiency (Verstraete and Vandevivere, 1999; Aiyuk et al., 2006). However, experimental studies have shown that by increasing the reactor temperature, the rate of anaerobic conversion and consequently the overall system efficiency can be improved (Matsushige et al., 1990; Viraraghavan and Varadarajan, 1996; Zakkour et al., 2001; Manariotis and Grigoropoulos 2003, 2006).

Heated packed-bed reactors are complex systems, which facilitate biological processes to occur at temperatures higher than ambient air temperatures. It should be noted that conventional heating of anaerobic low-strength wastewater reactors is not cost effective, because the typical volumes of wastewater treated are high. Recently, due to the rising cost of fuel, the use of solar energy for heating anaerobic reactors has become very attractive. Solar energy heating can offer a viable, environmentally friendly alternative to conventional heating practices, and can significantly contribute to the reduction of energy consumption.

In some regions, where there is plenty of sunshine throughout the year, solar energy is a relatively economical source for heating purposes. In such places, solar energy can be utilized for water heating, water distillation, desalination (Tiwari et al., 2003; Voropoulos et al., 2004), greenhouse heating, drying of sludge and agricultural products

* Corresponding author. Tel.: +30 2610 996 531; fax: +30 2610 996 573.
E-mail addresses: andyiann@teipat.gr (A.Ch. Yiannopoulos), I.D.Man@upatras.gr (I.D. Manariotis), gios@upatras.gr (C.V. Chrysikopoulos).

0960-8524/$ - see front matter © 2008 Elsevier Ltd. All rights reserved.
doi:10.1016/j.biortech.2008.01.067

either by direct sun exposure or by forced air circulation (Haralambopoulos et al., 2002; Akpinar, 2004; Santos et al., 2005), and heating of anaerobic waste treatment reactors (El-Mashad et al., 2003, 2004a,b; Wu and Bibeau, 2006).

Much of the previous research on solar reactor systems for waste treatment focused on the anaerobic digestion of manure. Axaopoulos et al. (2001) investigated the solar-heated anaerobic digestion of swine manure. The solar heated system that was employed consisted of a digester covered with flat-plate solar collectors, which were connected to a heat exchanger immersed in the manure. El-Mashad et al. (2003, 2004a,b) have studied the anaerobic digestion of cattle manure by two different types of completely stirred, thermophilic, anaerobic reactor systems. One system consisted of a solar collector placed outside of the reactor, and the other with a solar collector mounted on the reactor roof. The experimental investigations focused on the effects of temperature fluctuations, reactor size, and insulation characteristics on methane production. Wu and Bibeau (2006) developed a 3-D mathematical model to simulate the heat transfer from solar radiation incident to the cover of an anaerobic manure digester.

The aim of this paper was to investigate the design parameters for a solar-energy heated anaerobic-filter system for the treatment of municipal wastewater. It was demonstrated that a solar reactor for anaerobic treatment of low-strength wastewaters at elevated temperatures can lead to improved process performance and stability. Model simulations were performed for the meteorological conditions at four different geographical regions (i.e., France, Greece, Israel, and Sweden) to assess the heat efficiency of the newly designed solar anaerobic-filter system.

2. Methods

2.1. System configuration

The system considered in this study consisted of flat plate solar collectors, a heat exchanger, a warm water storage tank and an anaerobic filter (AF) reactor. Warm water from the storage tank and recirculated water from the reactor were mixed in appropriate volumetric fractions with the aid of a three-way tempering valve, so that the resulting mixture was maintained at a steady, pre-specified temperature. The liquid mixture was pumped into the twin-walls of the AF reactor. The main components of the solar reactor system are fully described in the following sections.

2.2. Anaerobic filter reactor

The AF reactor, as illustrated in Fig. 1, was a metallic cylindrical tank with a twin-wall enclosure. A network of inlet ports located at the bottom of the reactor distributed evenly the influent wastewater. The packing material was pebble. The bottom and cylindrical surfaces were well insulated. Heat dissipation to the ambient air was allowed from

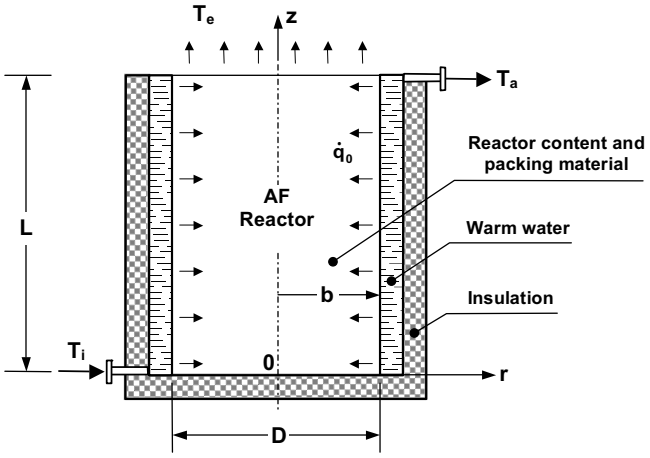

Fig. 1. Schematic diagram of the reactor model configuration showing the heat transfer processes.

Table 1
Classification of AF reactor types

Reactor type	Reactor dimensions			Reactor content thermal conductivity, λ (W m^{-1} K^{-1})
	Diameter, D (m)	Height, L (m)	Volume, V (m^3)	
A_1	1.20	1.80	2.04	0.6
A_2	1.20	1.80		2.0
B_1	2.50	4.00	19.63	0.6
B_2	2.50	4.00		2.0

the upper circular surface of the reactor. The warm water entered the reactor from a set of distributed inlets located at the base periphery and flowed through the void space of the twin-wall. The warm water exited the reactor from the upper periphery and flowed back to the storage tank. The AF reactor size as well as the type of packing material affected considerably the heat demand and size specifications of the solar system. For this study, only two different AF reactor volume sizes were examined and classified into four categories depending on the assumed thermal conductivity coefficient of their combined packing-wastewater material. The various AF reactor systems considered in this study are listed in Table 1.

2.3. Solar collectors and heat exchanger

An array of flat-plate collector modules, connected in parallel was employed to absorb sun rays. The solar collectors heated the circulating fluid, which was a mixture of water and ethylene-glycol of about 40% by weight. This mixture was selected in order to avoid possible freezing when ambient temperatures fell below zero. The solar collectors were coated with an absorptive surface, oriented to the south, and inclined at a preselected optimum angle. The design characteristics of the collectors (i.e., the net absorption surface of a single module, the energy loss product, and the energy absorption product) were obtained from

various manufacturers catalogues. A counter-flow heat exchanger unit was located next to the storage tank so that heat from the circulating fluid was easily transferred to the water of the storage tank.

2.4. Heat storage tank

Because the solar energy received by the solar collectors was temporally variable, an insulated cylindrical water tank was used to store the excess of heat for utilization during time periods with low or no sun radiation. Hot water from the heat storage tank was transferred to the AF reactor through a closed pipe system. The AF reactor energy demands were time dependent because the reactor heat losses were inversely proportional to the temporally variable ambient air temperature. Consequently, the stored energy was consumed only when there was a demand for heat in the AF reactor. From a calculation standpoint, the volume of the storage tank could be specified by the AF reactor size as well as by the weather conditions at the geographic region of the solar reactor system.

2.5. Meteorological data

In this study, model simulations were conducted for various fictitious solar reactor systems located at regions with distinctly different meteorological conditions. The four geographic regions selected were: Bet-Dagan, Israel; Paris, France; Patras, Greece; and Stockholm, Sweden.

The weather conditions at each location were essential to the solar system performance. Solar radiation as well as ambient air temperature data at the selected locations was generated on an hourly basis for a complete year by the software METEONORM (Remund et al., 1999). This software is essentially a meteorological database for climatology and solar energy. The solar collector inclination angle was also accounted for, because it greatly affects the collected average hourly radiation.

2.6. Solar collector inclination angle

The angle of the solar collector inclination was of primary importance because it controlled the amount of solar energy that can be collected. Consequently, the optimum solar collector inclination angle was determined for each geographic region selected. For a solar AF reactor system operated throughout the year, the optimum inclination angle of the solar collectors was assumed to be the one, which yielded maximum absorption of incident solar energy during the time period November through April. During this time period the heat demand by the solar AF reactor was most crucial. The sum of the solar energy collected over this period was calculated based on hourly values of irradiation provided by the METEONORM meteorological dataset as a function of solar collector inclination angle for each of the four selected locations with different latitudes. The estimated optimum collector slopes that lead to the maximum solar energy absorption over the specified time period were: 45° for Bet Dagan, Israel; 45° for Patras, Greece; 50° for Paris, France; 65° for Stockholm, Sweden.

3. Method of analysis

3.1. Modeling the heat distribution in the AF reactor

For constant warm water flow rate into the AF reactor at steady temperature, the heat flux from the inside cylindrical surface of the AF reactor, as illustrated in Fig. 1, was considered as uniform. Consequently, the heat transfer problem was treated as a two-dimensional, steady state, conduction problem. The temperature distribution within the AF reactor was independent of time, but a function of the cylindrical coordinates (r, z), where r is the radial coordinate and z is the vertical coordinate. Considering that $T(r,z) = T^*(r,z) + T_e$, where T is the temperature at location (r, z) within the AF reactor, T_e is the ambient air temperature, and T^* is a temperature above the ambient air temperature, the governing partial differential equation that describes the steady state heat distribution within the cylindrical AF reactor is given by (Carslaw and Jaeger, 1959; Özisic, 1980):

$$\nabla^2 T^*(r,z) = \frac{\partial^2 T^*(r,z)}{\partial r^2} + \frac{1}{r}\frac{\partial T^*(r,z)}{\partial r} + \frac{\partial^2 T^*(r,z)}{\partial z^2} = 0 \qquad (1)$$

The appropriate boundary conditions are

$$\frac{\partial T^*(r,0)}{\partial z} = 0 \qquad (2)$$

$$\lambda\frac{\partial T^*(r,L)}{\partial z} + hT^*(r,L) = 0 \qquad (3)$$

$$T^*(0,z) \neq \infty \qquad (4)$$

$$\lambda\frac{\partial T^*(b,z)}{\partial z} = \dot{q}_0 \qquad (5)$$

where λ is the thermal conductivity of the reactor content (wastewater and packing material), h is the heat transfer coefficient between the top surface and the ambient air, b is the inner radius of the reactor, $\dot{q}_0$ is a constant heat flux per unit area of the inside cylindrical surface of the reactor, and L is the height of the reactor. The boundary condition (Eq. (2)) indicates that the bottom surface of the reactor was insulated. Condition (Eq. (3)) describes the heat transfer by convection from the upper boundary surface into the ambient air. Condition (Eq. (4)) imposes that the temperature at the vertical axis passing through the center of the reactor must be finite. Finally, condition (Eq. (5)) prescribes a constant heat flux along the cylindrical surface of the reactor.

The governing partial differential Eq. (1) subject to the boundary conditions (Eqs. (2)–(5)) define an eigenvalue problem because of the finite reactor height and the non-homogeneous boundary condition (Eq. (5)). The analytical closed form solution to this boundary value problem was

obtained by the straightforward but laborious method of separation of variables (Kreyszig, 1993) in terms of an infinite series as follows:

$$T^*(\xi,\zeta) = \frac{4\dot{q}_0 L}{\lambda}\sum_{m=1}^{\infty} B_m \frac{I_0(\beta_m b\xi/L)}{I_1(\beta_m b/L)}\cos(\beta_m\zeta),\quad 0\le\xi\le 1,\ 0\le\zeta\le 1 \tag{6}$$

where I_0 and I_1 are the modified Bessel functions of order zero and order one, respectively, $\xi = r/b$ is the dimensionless radius, $\zeta = z/L$ is the dimensionless height, and B_m is given by

$$B_m = \frac{\sin\beta_m}{\beta_m[2\beta_m + \sin(2\beta_m)]} \tag{7}$$

and β_m's ($m = 1, 2, 3, \ldots$) are the positive roots of the following characteristic equation:

$$\beta_m \tan\beta_m = \frac{hL}{\lambda} \tag{8}$$

The roots of the characteristic equation were easily determined by the Newton–Raphson iterative procedure (Rao, 2002). It should be noted that no more than 100 roots of the characteristic equation were needed in order to achieve acceptable accuracy.

It was assumed that under steady state conditions the temperature of the reactor contents at the reactor bottom periphery was approximately equal to the warm water temperature at the reactor inlet. By setting $\xi = 1$, $\zeta = 0$, and $T^* = T - T_e \approx T_i - T_e$ in Eq. (6), the desired expression for the constant heat flux $\dot{q}_0$ becomes:

$$\dot{q}_0 = \frac{\lambda}{4L}(T_i - T_e)\left[\sum_{m=1}^{\infty} B_m \frac{I_0(\beta_m b/L)}{I_1(\beta_m b/L)}\right]^{-1} \tag{9}$$

It is more convenient to present the analytical solution Eq. (6) in terms of the inlet warm water temperature instead of $\dot{q}_0$. Thus, substituting Eq. (9) and $T^* = T - T_e$ into the analytical solution Eq. (6) yields the expression:

$$\frac{T - T_e}{T_i - T_e} = \left[\sum_{m=1}^{\infty} B_m \frac{I_0(\beta_m b\xi/L)}{I_1(\beta_m b/L)}\cos(\beta_m\zeta)\right] \times \left[\sum_{m=1}^{\infty} B_m \frac{I_0(\beta_m b/L)}{I_1(\beta_m b/L)}\right]^{-1},\quad 0\le\xi\le 1,\ 0\le\zeta\le 1 \tag{10}$$

3.2. Heat demand and dissipation

The total heat demand, Q_L, required by the solar reactor system designed here is:

$$Q_L = Q_r + Q_{Lr} + Q_{Ls} + Q_{Lp} \tag{11}$$

where $Q_r = \pi D L \dot{q}_0$ is the heat demand by the reactor content, $Q_{Lr} = (UA)_r(T_m - T_e)$ is the reactor heat losses from the insulated surfaces, $Q_{Ls} = (UA)_s(T_s - T'_e)$ is the warm water storage tank heat losses to the surroundings, $Q_{Lp} = (UA)_p(T_s - T_e)$ is the total heat losses from the pipe loop that circulated warm water between the storage tank and the AF reactor, and $(UA)_r$ is the heat transfer coefficient-area product for the reactor, $(UA)_s$ is the heat transfer coefficient-area product for the warm water storage tank, $(UA)_p$ is the heat transfer coefficient-area product for the warm water pipe loop, and T_m is the average temperature of the warm water within the twin-wall of the reactor, T_s is the temperature of the water in the storage tank, T'_e is the temperature of the warm water storage tank surroundings, which could be different than the ambient air temperature if the storage tank was placed indoors.

3.3. Water storage tank and reactor inlet temperature

The change of the uniform (fully mixed) warm water storage tank temperature over a time increment of $\Delta t = 1$ hour is estimated by the following expression:

$$T_s^+ = T_s + \frac{\Delta t}{(Mc_p)_s}(Q_u - Q_L) \tag{12}$$

where T_s and T_s^+ are the temperatures of the warm water in the storage tank at the beginning and end of the time increment Δt, Q_u is the useful energy gain of the solar collector, Q_L is the total heat demand given by Eq. (11), and $M = \rho V_s$ is the warm water storage tank capacity (where ρ is the water density, and V_s is the volume of the storage tank). In view of Eq. (12), the warm water storage tank temperature was calculated incrementally on an hourly basis. If $T_s < 20$ °C the warm water flow was interrupted, because it offered no useful energy, or if $T_s > 35$ °C the temperature of the warm water entering the AF reactor was tempered by a three-way valve so that its temperature was maintained at the specified upper limit of 35 °C (the optimum temperature). Consequently, the warm water inlet temperature to the reactor can be expressed as:

$$T_i = \begin{cases} 20°C, & T_s < 20°C \\ T_s, & 20 \le T_s \le 35°C \\ 35°C, & T_s > 35°C \end{cases} \tag{13}$$

3.4. Solar collector energy gain

The useful energy gain, Q_u, of the solar collector was estimated with the methods outlined by Sukhatme (1984) and Duffie and Beckman (1991). The useful energy gain was controlled by the solar collector area, A_c, and incident irradiation per unit area of the tilted solar collector, I_T, as well as with the characteristic features of the solar collector and heat exchanger listed in Table 2.

3.5. Effect of temperature on AF reactor performance

The experimental data collected by Manariotis and Grigoropoulos (2006) showed that the removal of chemical oxygen demand (COD) from raw municipal wastewater

Table 2
Parameter values for model simulations

Description	Value
General	
Heat transfer coefficient to ambient air[a]	24 (W m^{-2} K^{-1})
Thermal conductivity coefficient of insulation[a]	0.035 (W m^{-1} K^{-1})
AF reactor	
Twin-wall spacing	0.050 (m)
Thickness of insulation for types A_1 and A_2	0.080 (m)
Thickness of insulation for types B_1 and B_2	0.100 (m)
Solar collector	
Net absorption surface of a single module[b]	2.50 (m^2)
Angle of inclination	45°, 50°, 65°
Energy absorption product[b]	0.75 (–)
Energy loss product[b]	4.13 (W m^{-2} K^{-1})
Heat exchanger	
Heat transfer coefficient-area product for reactors A_1 and A_2	320 (W K^{-1})
Heat transfer coefficient-area product for reactors B_1 and B_2	540 (W K^{-1})
Fluid recirculation systems	
Density of ethylene glycol solution 40%, at 60 °C[c]	1030 (Kg m^{-3})
Density of water, at 60 °C[c]	985 (Kg m^{-3})
Specific heat of ethylene glycol solution 40%, at 60 °C[c]	3650 (J Kg^{-1} K^{-1})
Specific heat of water, at 60 °C[c]	4184 (J Kg^{-1} K^{-1})
Volumetric flow rate for collector test conditions[c]	15 (mL s^{-1} m^{-2})
Volumetric flow rate of glycol solution[c]	15 (mL s^{-1} m^{-2})
Volumetric flow rate in the heat exchanger-tank loop	20 (mL s^{-1} m^{-2})
Mass flow rate in the tank-reactor loop for reactors A_1 and A_2	0.050 (Kg s^{-1})
Mass flow rate in the tank-reactor loop for reactors B_1 and B_2	0.125 (Kg s^{-1})
Warm water storage tank ($V_s = 0.75$ m^3)	
Diameter	0.75 (m)
Height	1.80 (m)
Thickness of insulation	0.080 (m)
Warm water storage tank ($V_s = 1.50$ m^3)	
Diameter	0.98 (m)
Height	2.15 (m)
Thickness of insulation	0.100 (m)
Collector-heat-exchanger-tank pipe network	
Diameter for $A_c = 10$ m^2	0.022 (m)
Diameter for $A_c = 20$ m^2	0.035 (m)
Length for collector output branch	20 (m)
Length for collector input branch	20 (m)
Thickness of insulation	0.020 (m)
Tank-reactor loop pipe network	
Diameter	0.028 (m)
Length for each branch	25 (m)
Thickness of insulation	0.020 (m)

[a] Sprenger (1977).
[b] RetScreen® International (www.retscreen.net).
[c] Duffie and Beckman (1991).

within AF reactors increases with increasing temperature. To examine the effect of temperature on COD removal, the following relationship that describes the substrate concentration within an AF reactor treating low-strength synthetic wastewater at steady state conditions was considered (Matsushige et al., 1990):

$$\frac{S_e}{S_i} = \frac{1}{1 + kX(\mathrm{HRT})} \tag{14}$$

where S_i and S_e are the substrate concentrations in influent and effluent, respectively; X is the concentration of microorganisms or total suspended solids (TSS) in the reactor; HRT is the hydraulic retention time; and k is the temperature dependent first-order rate constant, which varied with temperature according to the Arrhenius relationship (Sawyer et al., 2003):

$$K_{(T_2)} = K_{(T_1)}\theta^{(T_2 - T_1)} \tag{15}$$

where $K_{(T_1)}$ and $K_{(T_2)}$ are the kinetic rates at temperatures of T_1 and T_2, respectively; and θ is the temperature coefficient. In view of equations (14) and (15), the COD removal was evaluated for various temperatures and HRT values using the following expression:

$$\text{COD removal}\ (\%) = \frac{S_i - S_e}{S_i} \times 100 \tag{16}$$

for $k_{(20)} = 7.1\times10^{-4}$ L/mg·d (Viraraghavan and Varadarajan, 1996), $\theta = 1.07$, and $X = 2000$ mg TSS/L. The results for COD removal suggested that the AF reactor performance was considerably improved with increasing temperature, with optimum temperature within the range 30–35 °C. For example at 20 °C the COD removal efficiency was 59%, whereas at 35 °C the removal efficiency increased to 80%.

4. Results and discussion

Although the proposed solar heated reactor system was designed to accommodate several types of anaerobic reactors, this study focused only on the AF reactor types listed in Table 1, and the model simulations were based on the model parameter values listed in Table 2.

The temperature distributions within the reactor were determined using Eq. (6) with a heat flux, $\dot{q}_0$, selected so that the temperature at the base of the reactor was approximately at 35 °C. The results showed that there was no considerable temperature variation at any horizontal cross-section of the cylindrical reactor. However, the temperature increased slightly with increasing ξ for every ζ considered. The simulation indicated also that λ and $\dot{q}_0$ did not significantly affect the general trend of the temperature distributions within the reactors.

Using the previous analysis the relationship between the incident irradiation per unit area on a tilted solar collector, I_T, and the useful energy gain per unit area of a solar collector, q_u, where $q_u = Q_u/A_c$, can be obtained as a function of time. Based on the parameter values listed in Table 2, I_T and q_u were calculated on an hourly basis for a complete year. The q_u values followed closely the time-dependent behavior of the corresponding I_T values, and that in Patras, Greece, with latitude 38.15° and a collector slope of 45°, there were only just a few days per year without useful energy. Fig. 2 presents the cumulative values of I_T, Q_u, and Q_L, indicated by $\langle I_T\rangle$, $\langle Q_u\rangle$ and $\langle Q_L\rangle$, respectively, over the time period of a full year for a solar reactor system in Patras, Greece. The I_T values produced by METEONORM software were cumulated on an hourly basis; whereas, Q_u and Q_L values were calculated using the parameter values of Table 2. The results showed that the cumulative $\langle Q_u\rangle$ was a substantial fraction of the cumulative $\langle I_T\rangle$. Furthermore, as indicated by the insert of Fig. 2, the trends of $\langle Q_u\rangle$ and $\langle Q_L\rangle$ were quite similar, which suggested that the total heat demand by the solar reactor system was adequately met by the useful energy gained by the solar collector.

Model simulations for a solar reactor system in Patras, Greece based on parameters values of Table 2 were conducted in order to compare the variation of the warm water storage tank temperature, T_s, for a solar reactor system in Patras, Greece, to the variation of the useful energy gain, Q_u, per unit area of the solar collector and the total heat demand, Q_L. The T_s values were calculated from Eq. (12), using the parameters of Table 2. The comparison indicated that T_s and Q_u exhibited significant daily fluctuations, whereas Q_L remained practically flat. Furthermore, the ambient air temperature, T_e, and warm water storage tank temperature, T_s, variation for different warm water tank sizes, V_s, were determined as a function of time. It should be noted that all T_e values were provided by the software METEONORM, and T_s values were determined by Eq. (12). Both T_e and T_s exhibited daily fluctuations; however, the amplitude of oscillation of T_s decreased with increasing warm water tank volume. This is an intuitive result because water temperature fluctuations were inversely proportional to the water volume.

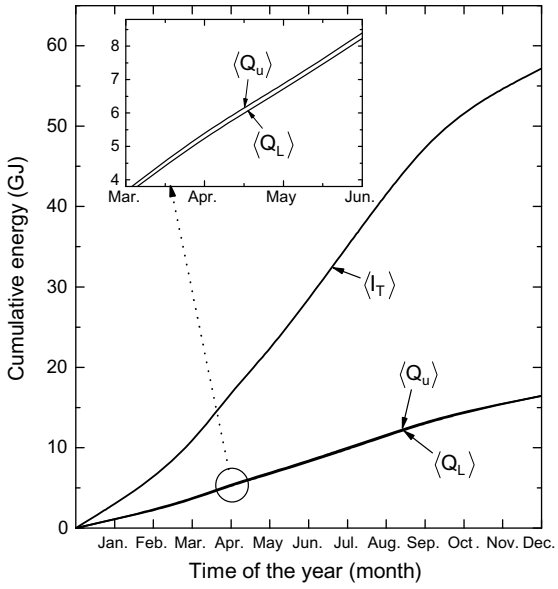

Fig. 2. Cumulative values $\langle I_T\rangle$, $\langle Q_u\rangle$ and $\langle Q_L\rangle$ for a solar reactor system in Patras, Greece. Here reactor type A_1, latitude = 38.15°, $A_c = 10$ m^2, $\beta = 45°$, and $V_s = 0.75$ m^3.

For convenience, the term "no-feed water period" was reserved in this study to represent the time period when warm water supply to the reactor was interrupted when the storage tank temperature was lower than 20 °C. The fraction of the year with no-feed water period, f, as a function of the warm water storage tank volume, for various solar collector sizes and reactor types based on the meteorological conditions of Patras, Greece was presented in Fig. 3. As expected, f decreased with increasing A_c and V_s for all reactor types considered. Note that for $A_c = 10$ m^2 and $V_s = 0.75$ m^3 and reactor types A_1 and A_2 the corresponding no-feed water periods were 1.2% and 1.8% of the year, respectively (see Fig. 3a). Also, for $A_c = 20$ m^2 and $V_s = 1.5$ m^3 and reactor types B_1 and B_2 the corresponding no-feed water periods were 0.25% and 0.41% of the year, respectively (see Fig. 3b). It should be noted that low f values characterised effective solar reactor systems. For the model simulations presented here, the ratio of the tank volume over the collector area (V_s/A_c) was set to 75 L/m^2, a value frequently used in many practical applications (Duffie and Beckman, 1991).

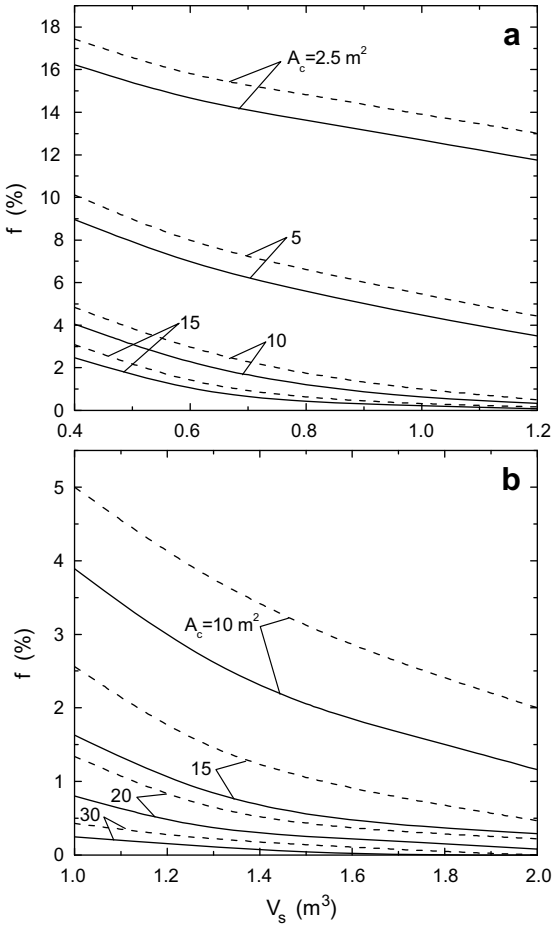

Fig. 3. Behavior of f as a function of V_s for various values of A_c based on meteorological conditions of Patras, Greece, for (a) reactor types A_1 (solid curves) and A_2 (dashed curves), and (b) reactor types B_1 (solid curves) and B_2 (dashed curves). Here latitude = 38.15°, and $\beta = 45°$.

For the meteorological conditions of Patras, Greece, hourly estimates of the water temperature at the reactor inlet, T_i, were calculated for a full year from Eq. (13). The results indicated that T_i remained at the upper limit of 35 °C throughout most of the year. There was only a small fraction of the year that the T_i was below 35 °C and just a few hours that remained close to 20 °C. The monthly averaged water temperature at the reactor inlet, $\bar{T}_i$, for a full year based on the meteorological conditions of Patras, Greece, for reactor types A_1 and A_2 with design parameters (as suggested by the results of Fig. 3): $A_c = 10\ m^2$, $\beta = 45°$, $V_s = 0.75\ m^3$; and reactor types B_1 and B_2 with design parameters: $A_c = 20\ m^2$, $\beta = 45°$, $V_s = 1.5\ m^3$ were presented in Fig. 4. The results suggested that, for every reactor type considered, $\bar{T}_i > 29$ °C all year long, and $\bar{T}_i \approx 35$ °C during the time period March through October. Clearly, the solar reactor system proposed here could easily be operated within the optimum temperature range (30–35 °C) as indicated by the AF reactor performance simulations for high COD removal.

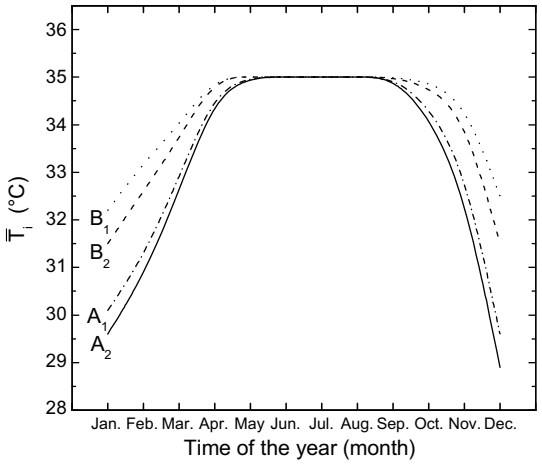

Fig. 4. Monthly average of water temperature at the reactor inlet as a function of time over a full year for reactor types A_1, A_2, B_1, and B_2. Here latitude = 38.15°, and $\beta = 45°$.

To gain a better understanding of the performance of the solar reactor system designed here, the hourly temperature of the warm water at the reactor inlet was calculated based on the meteorological conditions at four different geographic regions (Bet-Dagan, Israel; Paris, France; Patras, Greece; and Stockholm, Sweden) for reactor type A_1, with $A_c = 10\ m^2$, $V_s = 0.75\ m^3$ and the previously determined optimum collector slopes. The temperature range from 20 to 35 °C was divided into intervals of 5 °C. The number of hours that T_i fell within each of the 5 °C temperature increments was presented in days and tabulated in Table 3. The desired AF reactor operational temperature that yielded a COD removal of about 80% was 35 °C. Consequently, the results of Table 3 showed that the solar system was operated at the optimum temperature increment (30–35 °C) at Bet Dagan, Israel, for 363 days (99% of year without any no-feed water days, $T_i < 20$ °C), at Patras, Greece, for 316 days (87% of year and only 4.5 no-feed water days), at Paris, France, for 225 days (62% of year and 57 no-feed water days), and at

Table 3
Number of days of a full year that the simulated T_i remains within the specified temperature ranges

Reactor location	Range of water temperature at the reactor inlet, T_i			
	<20 °C	20–25 °C	25–30 °C	30–35 °C
Bet Dagan, Israel (lat. 32.00°)	0	0.5	1.5	363
Patras, Greece (lat. 38.15°)	4.5	21.5	23	316
Paris, France (lat. 49.12°)	57	42	41	225
Stockholm, Sweden (lat. 59.11°)	89	48	33	195

Stockholm, Sweden, for 196 days (54% of year and 89 no-feed water days). Note that in northern latitudes there was a decrease of optimum temperature days and an increase in no-feed water days. Clearly, the solar reactor system examined in this study could be satisfactorily operated in geographic regions with latitudes up to 50.00°. For greater latitudes the solar reactor system could be useful if the solar collector area and the warm water storage capacity could be increased considerably.

5. Conclusions

This work focuses on the design of a solar reactor system consisting of a solar collector, a heat exchanger, a warm water storage tank, and an AF reactor. The reactor was maintained at a desired operational temperature of 35 °C during the majority of the year. At this temperature the COD removal efficiency was approximately 80%. A mathematical model for the estimation of the heat demand or dissipation of every section of the solar system, as well as the steady state temperature distribution within the reactor was developed. Model simulations were conducted for numerous AF reactor types and various meteorological conditions representative of four different geographical areas (Bet-Dagan, Israel; Paris, France; Patras, Greece; and Stockholm, Sweden). The results suggested that efficient operation of the reactors considered could be achieved for latitudes up to 50.00°. From an environmental point of view, the proposed self-powered, solar heated reactor system could be economically attractive and environmentally friendly.

Acknowledgements

This work was sponsored by the Archimedes-EPEAK II Research Program, funded by the European Social Fund and National Resources. The content of this manuscript does not necessarily reflect the views of the agencies and no official endorsement should be inferred.

References

Akpinar, E.K., 2004. Experimental determination of convective heat transfer coefficient of some agricultural products in forced convection drying. International Communications in Heat and Mass Transfer 31, 585–595.

Aiyuk, S., Forrez, I., Lieven, D.K., van Haandel, A., Verstraete, W., 2006. Anaerobic and complementary treatment of domestic sewage in regions with hot climates—a review. Bioresource Technology 97, 2225–2241.

Axaopoulos, P., Panagakis, P., Tsavdaris, A., Georgakakis, D., 2001. Simulation and experimental performance of a solar-heated anaerobic digester. Solar Energy 70, 155–164.

Carslaw, H.S., Jaeger, J.C., 1959. Conduction of Heat in Solids, second ed. Oxford University Press.

Duffie, J.A., Beckman, W.A., 1991. Solar Engineering of Thermal Processes. John Wiley & Sons, Inc., New York.

El-Mashad, H.M., van Loon, W.K.P., Zeeman, G., 2003. A model of solar energy utilisation in the anaerobic digestion of cattle manure. Biosystems Engineering 84, 231–238.

El-Mashad, H.M., van Loon, W.K.P., Zeeman, G., Bot, G.P.A., Lettinga, G., 2004a. Design of a solar thermophilic anaerobic reactor for small farms. Biosystems Engineering 87, 345–353.

El-Mashad, H.M., Zeeman, G., van Loon, W.K.P., Bot, G.P.A., Lettinga, G., 2004b. Effect of temperature and temperature fluctuation on thermophilic anaerobic digestion of cattle manure. Bioresource Technology 95, 191–201.

Haralambopoulos, D.A., Biskos, G., Halvadakis, C., Lekkas, T.D., 2002. Dewatering of wastewater sludge through a solar still. Renewable Energy 26, 247–256.

Kreyszig, E., 1993. Advanced Engineering Mathematics, seventh ed. Wiley.

McCarty, P.L., 1982. One hundred years of anaerobic treatment. In: Hughes, D.E. et al. (Eds.), Anaerobic Digestion 1981. Proc. 2nd Int. Symposium on Anaerobic Digestion, Travemünde, Germany, 6-11 Sept. 1981. Elsevier, Amsterdam, pp. 3–22.

Manariotis, I.D., Grigoropoulos, S.G., 2003. Anaerobic treatment of low-strength wastewater in a biofilm reactor. Journal of Environmental Science and Health, Part A—Toxic/Hazardous Substances & Environmental Engineering 38, 2057–2068.

Manariotis, I.D., Grigoropoulos, S.G., 2006. Municipal-wastewater treatment using upflow-anaerobic filters. Water Environmental Research 78, 233–242.

Matsushige, K., Inamori, Y., Mizuochi, M., Hosomi, M., Sudo, R., 1990. The effects of temperature on anaerobic filter treatment for low-strength organic wastewater. Environmental Technology 11, 899–910.

Metcalf, Eddy, 2003. Wastewater engineering: treatment and reuse, fourth ed. Revised by G. Tchobanoglous, F.L. Burton and H.D. Stensel, McGraw-Hill.

Özisic, M.N., 1980. Heat Conduction. John Wiley & Sons, New York.

Rao, S.S., 2002. Applied Numerical Methods for Engineers and Scientists. Prentice Hall.

Remund, J., Kunz, S., Lang, R., 1999. METEONORM, Global Meteorological Database for Solar Energy and Applied Climatology, Solar Engineering Handbook, Version 4. Meteotest, Bern, Switzerland.

RetScreen® International, Clean Energy Decision Support Center, Clean Energy Project Analysis Tools. Natural Resources, Canada (www.retscreen.net).

Santos, B.M., Queiroz, M.R., Borges, T.P.F., 2005. A solar collector design procedure for crop drying. Brazilian Journal of Chemical Engineering 22, 277–284.

Sawyer, C.N., MacCarthy, P.L., Parkin, G.F., 2003. Chemistry for Environmental Engineering and Science, fifth ed. Mc Graw Hill.

Sprenger, E., 1977. Taschenbuch für Heizung und Klimatechnik. R. Oldenbourg Verlag GmbH, München.

Sukhatme, S.P., 1984. Solar Energy: Principles of Thermal Collection and Storage. McGraw-Hill.

Switzenbaum, M.S., 1995. Obstacles in the implementation of anaerobic treatment technology. Bioresource Technology 53, 255–262.

Tiwari, G.N., Singh, H.N., Tripathi, R., 2003. Present status of solar distillation. Solar Energy 75, 367–373.

Verstraete, W., Vandevivere, P., 1999. New and broader applications of anaerobic digestion. Critical Review in Environmental Science Technology 28, 151–173.

Viraraghavan, T., Varadarajan, R., 1996. Low-temperature kinetics of anaerobic-filter wastewater treatment. Bioresource Technology 57, 165–171.

Voropoulos, K., Mathioulakis, E., Belessiotis, V., 2004. A hybrid solar desalination and water heating system. Desalination 164, 189–195.

Wu, B., Bibeau, E.L., 2006. Development of 3-D anaerobic digester heat transfer model for cold weather applications. Transactions of the American Society of Agricultural and Biological Engineers (ASABE) 49, 749–757.

Zakkour, P.D., Gaterell, M.R., Griffin, P., Gochin, R.J., Lester, J.N., 2001. Anaerobic treatment of domestic wastewater in temperature climates: treatment plant modeling with economic considerations. Water Research 35, 4137–4149.